JSR Publications

Available Online

J. Sci. Res. **18** (1), 107-122 (2026)

JOURNAL OF SCIENTIFIC RESEARCH

www.banglajol.info/index.php/JSR

Dynamics of Cosmic String and Domain Wall Cosmological Model with a Special Form of Deceleration Parameter

V. G. Mete[1], S. N. Bayaskar [2], A. A. Dhanagare[2,*], A. A. Jalamkar[1]

[1]Department of Mathematics, R.D.I.K. & N. K.D. College, Badnera-Amravati 444701, India

[2]Department of Mathematics, Adarsha Science, J. B. Art and Birla Commerce College, Dhamangaon Rly, Dist. Amravati 444 709, India

Received 18 June 2025, accepted in final revised form 30 October 2025

Abstract

In the present work, the Bianchi Type III spacetime is taken into account in the presence of a cosmic string and a domain wall within the framework of $f(R,T)$ theory of gravitation. A specific form of the $f(R,T)$, theory, namely $f(R,T) = R + 2f(T)$, is taken into account in this work. The modified field equations for cosmic string and domain wall models are solved using a particular form of the deceleration parameter, and their physical behaviors are analyzed. In addition, the EoS parameter, jerk parameter, statefinder pair, and $Om(z)$ diagnostic are utilized to analyze the evolutionary behavior of the Universe under the considered modified gravity model, indicating a quintessence-type nature of the cosmic expansion.This research offers significant insights into the anisotropic behaviour of the Universe and effectively describes the cosmic acceleration observed during late times. Our findings are then compared to recent observational data and are found to be in agreement with the ΛCDM model.

Keywords: (R,T) Gravity; Cosmic string; Domain Wall; Bianchi type III.

doi: https://dx.doi.org/10.3329/jsr.v18i1.82279 J. Sci. Res. **18** (1), 107-122 (2026)

1. Introduction

The early Universe remains one of the most captivating subjects in cosmology, holding the key to unravelling the mysteries of its origin and evolution. Einstein's General Theory of Relativity, a cornerstone of modern physics, has profoundly shaped our understanding of cosmic dynamics and the large-scale structure of the Universe. However, the complexities of the early Universe, including the phase transitions that led to the formation of topological defects such as cosmic strings and domain walls, demand deeper investigation. The last two decades have marked a turning point in cosmology, as compelling observations from Type Ia supernovae [1-3] and the cosmic microwave background (CMB) [4] reveal an accelerating Universe. Moreover, studies on Baryon Acoustic Oscillations [5,6], Wilkinson Microwave Anisotropy Probe [7], the large-scale structure of the universe [8,9], assessments of galaxy redshifts [10], and examinations of the CMB radiation (CMBR)

* *Corresponding author*: dhanagarea1995@gmail.com

[11,12] all provide convincing empirical proof for this phenomenon. This revelation not only challenges Einstein's original framework but also beckons us toward a deeper understanding of the forces shaping our cosmic destiny.

The study of cosmic strings and domain walls has garnered significant interest in cosmology due to their critical role in the formation of structures and the evolution of the Universe. These entities are topological defects that come out as a result of spontaneous symmetry breaking, typically during phase transitions in the early Universe. The gravitational influences of cosmic strings have been extensively explored in works by Vilenkin [13], Letelier [14], Satchel [15], and Adhav *et al*. [16, 17] within the framework of general relativity.

Cosmic strings are one-dimensional topological defects that may have formed during the early Universe's phase transitions. These are comparable to 'cracks' in spacetime resulting from spontaneous symmetry breaking in a high-energy field. Cosmic strings tell us about the observable effects of extreme energy densities and gravitational lensing, the formation of large-scale structures like galaxies and clusters. It provides a testbed for understanding the dynamics of symmetry-breaking mechanisms in the early Universe. Some distinguishing features of cosmic strings are, they are extremely thin but incredibly dense, with masses that could stretch across vast cosmic scales, Capable of producing gravitational lensing effects, bending light from distant sources, their oscillations and decay can generate gravitational waves, potentially detectable by modern observatories. Reddy [18,19] has obtained string cosmological models in Brans-Dicke and Saez-Ballester scalar tensor theories of gravitation when the sum of the energy density and the tension density of the cosmic string source vanish. String cosmological models in alternative theories of gravitation have been investigated by several authors [20-24]. Reddy and Naidu [25,26] analysed the cosmic strings with $f(R,T)$ gravity theory and their analysis revealed the absence of viable cosmic string and perfect fluid configurations in this particular theory. Pawar *et al*. [27] Examined the behaviour of string cosmological model incorporating a massless scalar field within the framework of a modified theory of general relativity. Bianchi type VI_0 space-time was investigated by Pawar [28] in the presence of a cloud of strings coupled with a perfect fluid within the framework of $f(R,T)$ gravity. Chirde *et al*. [29] investigated the LRS Bianchi type I metric with the source as barotropic perfect fluid and cosmic string in the framework of $f(T)$ gravity using three different functional forms of $f(T)$ gravity. Kantowaski-Sachs cosmological model with viscous cosmic string in the quadratic form of teleparallel gravity for a particular choice of $f(T)$ formalism was studied by Bhoyar et al. [30].

Domain walls are two-dimensional topological defects that arise when a discrete symmetry is spontaneously broken during a phase transition. They can be visualized as 'boundaries' separating regions with different vacuum states. Unlike cosmic strings, domain walls are extended structures with large surface energy densities. Their gravitational effects are significant, but their persistence could disrupt the observed Universe, requiring mechanisms to limit their abundance. Their presence could manifest in gravitational waves, CMB anisotropies, or deviations in galaxy distributions. While talking about Topological

Stability of domain wall, Domain walls are stable due to their topological nature, arising from the vacuum manifold's configuration during symmetry breaking. Hill et al. proposed that domain walls are important in the formation of galaxies. Domain walls have gained significant attention in recent years from a cosmological perspective, particularly due to their role in newly proposed scenarios of galaxy formation. According to the researcher the formation of galaxies is due to domain walls produced during phase transitions after the time of recombination of matter and radiation. The study of Thick Domain Walls in Brans-Dicke Theory of Gravitation was done by Pawar and Bayaskar [31]. Some authors have investigated domain walls in alternative theories of gravitation, one can refer [32-35]. Rao et.al. discussed Kantowski-Sachs Models with Domain Walls in $f(R,T)$ Theory of Gravity [36], Katore, Hatkar et.al. studied domain wall with different theories, $f(R,T), f(Q)$[37-41]. "Comparative study of transition FLRW and axially symmetric cosmological structures with domain walls in f (R, T) gravity" was done by Sharma *et al.* [42]. Pawde [43] studied Anisotropic behavior of universe in $f(R,L_m)$ gravity using special form of deceleration parameter. Same form was used by other also [48,49]. Mete *et al.* [53,54] studied five-dimensional cosmological model with one-dimensional cosmic string coupled with zero mass scalar field in Lyra manifold and qualitative behavior of cosmological model with cosmic strings and minimally interacting dark energy. Bayaskar *et al.* [55] studied logarithmic $f(Q)$ gravity with parametrization of deceleration parameter and energy conditions. Ugale *et al.* [56] studied anisotropic Bianchi Type VI_0 cosmological models in a modified $f(R,T)$ gravity.

Cosmic strings, with their linear structure, and domain walls, characterized by their two-dimensional nature, are not merely theoretical constructs but are believed to have played a pivotal role in shaping the Universe's evolution. Both Cosmic string and domain wall was discussed by several authors [44-46]. Inspired by the aforementioned motivations this study concentrates on exploring these entities within the framework of $f(R,T)$ theory. The physical and geometrical aspects of the models are also studied with their graphical behaviour.

The current manuscript is organised as follows: Section 2 provides the brief Overview of $f(R,T)$ gravity. In section 3 the metric and field equations of both cosmic string and domain wall are derived. Cosmological Solution for $f(R,T)$ gravity with some parameters discussed in section 4. Some Dynamical properties are in section 5. Graphs and their observation are given in section 6. In section 7 we conclude the present work.

2. Overview/ Formalism of $f(R,T)$ Gravity

Harko *et al*. [50] proposed another modification of Einstein's theory of gravitation which is known as $f(R,T)$ theory of gravity. Wherein the gravitational Lagrangian is given by an arbitrary function of the Ricci scalar *R* and of the trace T of the stress energy tensor T_{ij}. Using the Hilbert–Einstein approach, the field equations for $f(R,T)$ gravity are derived from the total action introduced by Harko *et al.* [50] as:

$$S = \int \left[\frac{1}{2k} f(R,T) + L_m\right] \sqrt{-g}\ d^4x \tag{1}$$

where, $k = 8\pi G$, g is the determinant of the metric, L_m is the matter Lagrangian density, $f(R,T)$ is the arbitrary function of the scalar curvature R and the trace T of the energy momentum tensor T_{ij} .

The energy–momentum tensor T_{ij} corresponding to the matter source is taken in the form:

$$T_{ij} = \frac{-2}{\sqrt{-g}} - \frac{\delta(\sqrt{-g}\,L_m)}{\delta\, g^{ij}} \tag{2}$$

where its trace is given by $T = g^{ij}T_{ij}$

By differentiating the action Eq. (1) of the gravitational field with respect to the metric tensor g_{ij}, Consequently, the field equations governing $f(R,T)$ gravity take the form:

$$f_R(R,T)R_{ij} - \frac{1}{2}f(R,T)g_{ij} + \left(g_{ij}\square - \nabla_i\nabla_j\right)f_R(R,T) = kT_{ij} - f_T(R,T)T_{ij} - f_T(R,T)\theta_{ij} \tag{3}$$

where, $f_R(R,T) = \frac{\partial f(R,T)}{\partial R}$, $f_T(R,T) = \frac{\partial f(R,T)}{\partial T}$, $\theta_{ij} = g^{mn}\frac{\delta T_{mn}}{\delta g^{ij}}$, $\square = \nabla^i\nabla_j$

$\nabla_i\nabla_j$ denotes the covariant derivative.

Here c is the speed light in vacuum and the Newtonian gravitational constant is G. The stress–energy tensor of the matter distribution is considered in the form:

$$T_{ij} = (\rho + p)u_iu_j - pg_{ij} \tag{4}$$

In accordance with a basic statement of fluid mechanics, the matter Lagrangian density L_m is related to the fluid pressure through the relation L_m = - p.

$$u^i\nabla_j u_i = 0\,,\ u^iu_i = 1 \tag{5}$$

By using the above value of θ_{ij}, we get the variation of stress energy of perfect fluid as,

$$\theta_{ij} = -2T_{ij} - pg_{ij} \tag{6}$$

The different forms of matter distribution will yield different theoretical models of $f(R,T)$ gravity However, Harko *et al.* [50] have obtained three particular classes of $f(R,T)$ gravity models as

$$f(R,T) = \begin{Bmatrix} R + 2f(T) \\ f_1(R) + f_2(T) \\ f_1(R) + f_2(R)f_3(T) \end{Bmatrix} \tag{7}$$

Here we take,

$$f(R,T) = R + 2f(T) \tag{8}$$

For this particular choice of $f(R,T)$, from (3), we get the field equation as

$$R_{ij} - \frac{1}{2}R\,g_{ij} = 8\pi T_{ij} - 2f'(T)\,T_{ij} - 2f'(T)\,\theta_{ij} + f(T)g_{ij} \tag{9}$$

The value of θ_{ij} given in Eq. (6) and above equation gives us a field equation in the form

$$R_{ij} - \frac{1}{2}R\,g_{ij} = 8\pi T_{ij} + 2f'(T)\,T_{ij} + 2pf'(T)\,g_{ij} + f(T)g_{ij} \tag{10}$$

where $f'(T)$ is the differentiation of $f(T)$ with respect to the argument T.

3. Metric and Field Equation

The Universe is considered to possess a spatially homogeneous and anisotropic geometry described by the Bianchi Type III metric of the form:

$$ds^2 = dt^2 - A^2dx^2 - B^2e^{2x}dy^2 - C^2dz^2 \tag{11}$$

where $A, B,$ and C are the functions of cosmic time $'t'$ only.

3.1. *Cosmic string*

The energy-momentum tensor for cosmic string (Letelier [51]) is given by,

$$T_{ij} = \rho\, u_i u_j - \lambda\, x_i x_j \tag{12}$$

where, ρ is the rest energy density of the system, λ is the tension density of the cosmic string,

The component of comoving four velocity vector in cosmic fluid is $u^i = (0,0,0,1)$ with $u_i u^j = 0$ and

$$g_{ij} u^i u_j = -x^i x_j = -1,\ \ u^i x_i = 0 \tag{13}$$

Using comoving coordinates system and a particular choice of the function given by Harko et al. [50] we take the function $f(T)$ as,

$$f(T) = \mu T \tag{14}$$

where, μ is constant.

Now, by assuming the commoving coordinate system, the field Eq. (10) for the metric given by Eq. (11) using the Eqs. (12) - (14) the field equations become

$$\frac{\ddot{B}}{B} + \frac{\ddot{C}}{C} + \frac{\dot{B}\dot{C}}{BC} = -(2p\mu + \mu\lambda + \mu\rho) \tag{15}$$

$$\frac{\ddot{A}}{A} + \frac{\ddot{C}}{C} + \frac{\dot{A}\dot{C}}{AC} = -(2p\mu + \mu\lambda + \mu\rho) \tag{16}$$

$$\frac{\ddot{A}}{A} + \frac{\ddot{B}}{B} + \frac{\dot{B}\dot{A}}{BA} + \frac{1}{A^2} = -(8\pi\lambda + 3\mu\lambda + 2p\mu + \mu\rho) \tag{17}$$

$$\frac{\dot{A}\dot{B}}{AB} + \frac{\dot{A}\dot{C}}{AC} + \frac{\dot{B}\dot{C}}{BC} + \frac{1}{A^2} = -(8\pi\rho + 3\mu\rho + 2p\mu + \mu\lambda) \tag{18}$$

$$\frac{\dot{B}}{B} - \frac{\dot{A}}{A} = 0 \tag{19}$$

An overhead dot (·) shows the derivative with respect to cosmic time t.

From Eq. (19) we get, $A = mB$, for the sake of simplicity take $m = 1$, we get

$$A = B \tag{20}$$

Using Eq. (20), Eq. (15) – (18) become

$$\frac{\ddot{B}}{B} + \frac{\ddot{C}}{C} + \frac{\dot{B}\dot{C}}{BC} = -(2p\mu + \mu\lambda + \mu\rho) \tag{21}$$

$$\frac{\ddot{B}}{B} - \frac{\ddot{C}}{C} + \frac{\dot{B}^2}{B^2} - \frac{\dot{B}\dot{C}}{BC} + \frac{1}{B^2} = (-8\pi - 2\mu)\lambda \tag{22}$$

$$\frac{\dot{B}^2}{B^2} + \frac{\dot{B}\dot{C}}{BC} - \frac{\ddot{B}}{B} - \frac{\ddot{C}}{C} + \frac{1}{B^2} = (-8\pi - 2\mu)\rho \tag{23}$$

3.2. *Domain wall*

The energy-momentum tensor for Domain wall is given by

$$T_{ij} = \rho\left(g_{ij} + \omega_i\omega_j\right) + p\ \omega_i\omega_j \tag{24}$$

where p and ρ are the pressure and density of the fluid respectively and ω_i is four velocity vectors satisfying $\omega_i\omega^j = 0$ and $\omega_i\omega^i = -1$.

Now, by assuming the commoving coordinate system, the field Eq. (10) for the metric given by Eq. (11) using the Eqs. (14) and (24) the field equations become

$$-\left(\frac{\ddot{B}}{B} + \frac{\ddot{C}}{C} + \frac{\dot{B}\dot{C}}{BC}\right) = (8\pi + 5\mu)\rho + \mu p \tag{25}$$

$$-\left(\frac{\ddot{A}}{A} + \frac{\ddot{C}}{C} + \frac{\dot{A}\dot{C}}{AC}\right) = (8\pi + 5\mu)\rho + \mu p \tag{26}$$

$$-\left(\frac{\ddot{A}}{A}+\frac{\ddot{B}}{B}+\frac{\dot{B}\dot{A}}{BA}+\frac{1}{A^2}\right)=-(8\pi+\mu)p+3\mu\rho \tag{27}$$

$$-\left(\frac{\dot{A}\dot{B}}{AB}+\frac{\dot{A}\dot{C}}{AC}+\frac{\dot{B}\dot{C}}{BC}+\frac{1}{A^2}\right)=(8\pi+5\mu)\rho+\mu p \tag{28}$$

$$\frac{\dot{B}}{B}-\frac{\dot{A}}{A}=0 \tag{29}$$

An overhead dot (·) shows the derivative with respect to cosmic time t.

From Eq. (29) we get, we get, $A=mB$, for the sake of simplicity take $m=1$, yields

$$A=B \tag{30}$$

Using Eq. (30), Eqs. (25) - (28) becomes

$$-\left(\frac{\ddot{B}}{B}+\frac{\ddot{C}}{C}+\frac{\dot{B}\dot{C}}{BC}\right)=(8\pi+5\mu)\rho+\mu p \tag{31}$$

$$-\left(\frac{2\ddot{B}}{B}+\frac{\dot{B}^2}{B^2}+\frac{1}{B^2}\right)=-(8\pi+\mu)p+3\mu\rho \tag{32}$$

$$-\left(\frac{\dot{B}^2}{B^2}+\frac{2\dot{B}\dot{C}}{BC}+\frac{1}{B^2}\right)=(8\pi+5\mu)\rho+\mu p \tag{33}$$

4. Cosmological Solution for $f(R,T)$Gravity with Some Parameters

In both of the cases discussed above, a system of three equations is obtained involving four unknowns. To solve the system of equation we have to consider an additional plausible condition to find the explicit solution for this system of equations.

In this particular study we use special form of deceleration parameter defined by Singh and Debnath [47] given by,

$$q=\frac{-a\ddot{a}}{\dot{a}^2}=-1+\frac{\eta}{1+a^{\eta}} \tag{34}$$

The sign of the parameter q in the model indicates whether the Universe is expanding or inflating. When $q>0$, it corresponds to a standard decelerating model, while $q<0$ suggests an accelerating expansion. It is important to mention that current observations, such as those from Type Ia Supernovae (SNe-Ia) and the CMBR, generally favor accelerating models with $q<0$, although neither observation alone fully determines this.

Solving Eq. (34) the Hubble parameter (H) is obtained as:

$$H=\frac{\dot{a}}{a}=\kappa(1+a^{-\eta}) \tag{35}$$

where, κ is constant of integration.

The scale factor holds significant importance in cosmology, serving as a key element in understanding the late-time dynamics and ultimate fate of the Universe. It is essential for describing the Universe's expansion and its interaction with dark energy, forming the backbone of modern cosmological models. Furthermore, the scale factor provides critical insights into the evolution of cosmic structures and it helps to understand the different stages in the Universe's history, from the early inflationary phase to the current accelerated expansion.

Therefore, integrating Eq. (35) we get the average scale factor (a) as

$$a=(e^{\eta t}-1)^{\frac{1}{\eta}} \tag{36}$$

Let us define some cosmologically important parameters, which are helpful for the physical and kinematical analysis of the solution.

The average scale factor $a(t)$ of the Bianchi type III space-time is defined as

$$a(t) = (ABC)^{\frac{1}{3}} \tag{37}$$

The spatial volume V of the metric is given by

$$V = a^3(t) = ABC$$

$$V = (e^{\eta t} - 1)^{\frac{3}{\eta}} \tag{38}$$

The directional Hubble parameter is given by

$$H_1 = \frac{\dot{A}}{A} = \frac{e^{\eta t}}{2(e^{\eta t}-1)} \qquad H_2 = \frac{\dot{B}}{B} = \frac{e^{\eta t}}{2(e^{\eta t}-1)} \qquad H_3 = \frac{\dot{C}}{C} = \frac{2e^{\eta t}}{(e^{\eta t}-1)} \tag{39}$$

The average Hubble parameter H is given by

$$H = \frac{1}{3}(H_1 + H_2 + H_3) = \frac{1}{3}\left(\frac{\dot{A}}{A} + \frac{\dot{B}}{B} + \frac{\dot{C}}{C}\right)$$

$$H(t) = \frac{e^{\eta t}}{(e^{\eta t}-1)} \;\&\; H(z) = \frac{H_0}{2}\,(1 + (1+z)^{\eta}) \tag{40}$$

The scalar expansion θ is given by

$$\theta = 3H = \left(\frac{\dot{A}}{A} + \frac{\dot{B}}{B} + \frac{\dot{C}}{C}\right)$$

$$\theta = \frac{3e^{\eta t}}{(e^{\eta t}-1)} = \frac{3H_0}{2}\,(1 + (1+z)^{\eta}) \tag{41}$$

The deceleration parameter is given by,

$$q(t) = -1 + \frac{\eta}{e^{\eta t}} \;\&\; q(z) = -1 + \frac{\eta}{1+\left(\frac{1}{1+z}\right)^{\eta}} \tag{42}$$

The mean anisotropic parameter Δ is given by

$$\Delta = \frac{1}{3}\ \sum_{i=1}^{3}\left(\frac{H_i - H}{H}\right)^2$$

$$\Delta = \frac{1}{2} \tag{43}$$

The Shear scalar σ^2 is given by

$$\sigma^2 = \frac{1}{2}\left(\frac{\dot{A}^2}{A^2} + \frac{\dot{B}^2}{B^2} + \frac{\dot{C}^2}{C^2}\right) - \frac{1}{6}\,\theta^2$$

$$\sigma^2 = \frac{3}{4}\left(\frac{e^{\eta t}}{(e^{\eta t}-1)}\right)^2 = \frac{3H_0}{8}\,(1 + (1+z)^{\eta}) \tag{44}$$

Now by using the above equation and the relation between spatial volume in terms of average scale factor the corresponding metric potentials A and B are obtained as,

$$A = B = (e^{\eta t} - 1)^{\frac{1}{2\eta}},\ C = (e^{\eta t} - 1)^{\frac{2}{\eta}} \tag{45}$$

Corresponding to above metric potentials, Eq. (11) yields

$$ds^2 = dt^2 - (e^{\eta t} - 1)^{\frac{1}{\eta}}dx^2 - (e^{\eta t} - 1)^{\frac{1}{\eta}}e^{2x}dy^2 - (e^{\eta t} - 1)^{\frac{4}{\eta}}\,dz^2 \tag{46}$$

4.1. *Jerk parameter*

In cosmology, the jerk parameter is a dimensionless quantity that measures how the acceleration of the universe's expansion changes over time. As a higher-order derivative of the scale factor $a(t)$, it goes beyond the Hubble parameter (which describes the expansion rate) and the deceleration parameter (which measures the change in the expansion rate) to provide a deeper understanding of the Universe's dynamics. The jerk parameter offers valuable insights into the dynamics of dark energy, the mysterious force driving the accelerated expansion of the Universe. By examining this parameter, researchers can explore potential transitions in the Universe's expansion phases, such as shifts between

acceleration and deceleration, shedding light on the evolution and future behavior of cosmic expansion.

The jerk parameter (j), can be defined as follows:

$$j = \frac{\ddot{a}}{aH^3} \tag{47}$$

By using Eqs. (36) and (40) in above equation we get,

$$j = 1 + \frac{\eta^2}{e^{\eta t}} + \frac{\eta^2}{e^{2\eta t}} - \frac{3\eta}{e^{\eta t}} \tag{48}$$

$$j = 1 + \frac{\eta^2}{\left(\frac{1}{1+z}\right)^{\eta}+1} + \frac{\eta^2}{\left(\left(\frac{1}{1+z}\right)^{\eta}+1\right)^2} - \frac{3\eta}{\left(\frac{1}{1+z}\right)^{\eta}+1} \tag{49}$$

4.2. *Statefinder parameter*

The statefinder parameters are dimensionless quantities designed to provide a deeper understanding of dark energy models and their influence on the Universe's expansion. These parameters enhance the analysis beyond the Hubble parameter (H) and the deceleration parameter (q), offering a more detailed picture of the expansion dynamics. By analyzing these parameters, researchers can gain deeper insights into the nature of dark energy and its impact on the evolution of the universe. Usually, the statefinder parameters are denoted as (r, s). They are particularly useful for distinguishing between different cosmological models, such as the Cold Dark Matter with a Cosmological Constant (ΛCDM) model and the Standard Cold Dark Matter (SCDM) model, by identifying unique fixed points (r, s) = (1, 0) and (r, s) = (1, 1) respectively correspond to each model's properties. They are defined in terms of higher-order derivatives of the scale factor a(t).

$$r = \frac{\ddot{a}}{aH^3} \text{ and } s = \frac{r-1}{3\left(q-\frac{1}{2}\right)} \tag{50}$$

By using Eqs. (36) and (40) in above equation we get,

$$r = 1 + \frac{\eta^2}{e^{\eta t}} + \frac{\eta^2}{e^{2\eta t}} - \frac{3\eta}{e^{\eta t}} \text{ and } s = \frac{2\eta^2\left(\frac{1}{e^{\eta t}}+1\right)-6\eta}{6\eta-9e^{\eta t}} \tag{51}$$

$$r = 1 + \frac{\eta^2}{\left(\frac{1}{1+z}\right)^{\eta}+1} + \frac{\eta^2}{\left(\left(\frac{1}{1+z}\right)^{\eta}+1\right)^2} - \frac{3\eta}{\left(\frac{1}{1+z}\right)^{\eta}+1} \text{ and } s = \frac{2\eta^2\left(\frac{1}{\left(\frac{1}{1+z}\right)^{\eta}+1}+1\right)-6\eta}{6\eta-9\left(\frac{1}{1+z}\right)^{\eta}+1} \tag{52}$$

4.3. $O_m(z)$ *Diagnostic parameter*

The O_m diagnostic, combining the Hubble parameter and redshift, introduced by Sahni [52] serves as a valuable tool to distinguish between dark energy models and the standard ΛCDM framework. It is a model-independent diagnostic, making it particularly useful for distinguishing ΛCDM from alternative dark energy models.

- **ΛCDM**: $O_m(z)$ remains constant across redshifts because dark energy behaves as a cosmological constant.
- **Quintessence**: $O_m(z)$ decreases with redshift due to the dynamic nature of the scalar field driving dark energy.

- **Phantom Energy**: $O_m(z)$ increases with redshift, reflecting the more extreme behavior of the equation of state ($\omega < -1$).

The $O_m(z)$ diagnostic, in parallel with statefinder parameters (r, s), offers a robust framework for understanding the nature of dark energy and the cosmic expansion history. This diagnostic is particularly effective in probing the present matter density contrast and the evolution of dark energy. The $O_m(z)$ parameter is defined as:

$$O_m(z) = \frac{\left[\frac{H(z)}{H_0}\right]^2 - 1}{(1+z)^3 - 1} \tag{53}$$

where $H(z)$ is the Hubble parameter at redshift z, and H_0 is the current Hubble constant. From Eq. (40), Eq. (53) becomes,

$$O_m(z) = \frac{[(1+z)^\eta + 3][(1+z)^\eta - 1]}{4\,[(1+z)^3 - 1]} \tag{54}$$

5. Some Dynamical Properties

5.1. *Cosmic string*

From Eqs. (21), (22), and (23) the string tension density is obtained as:

$$\lambda = \frac{-1}{(8\pi+2\mu)}\left[\frac{e^{2\eta t}}{(e^{\eta t}-1)^2}\left(\frac{3\eta}{2} - \frac{15e^{\eta t}}{4} - \frac{3}{4}\right) + \frac{1}{(e^{\eta t}-1)^{\frac{1}{\eta}}}\right] \tag{55}$$

$$\lambda = \frac{-1}{(8\pi+2\mu)}\left\{\left(\frac{1}{1+z}\right)^{-2\eta}\left(\left(\frac{1}{1+z}\right)^{\eta} + 1\right)^2\left(\frac{3\eta}{2} - \frac{15}{4}\left(\frac{1}{1+z}\right)^{\eta} - \frac{9}{2}\right) + (1+z)\right\} \tag{56}$$

Energy density as,

$$\rho = \frac{-1}{(8\pi+2\mu)}\left[\frac{e^{2\eta t}}{(e^{\eta t}-1)^2}\left(\frac{5\eta}{2} - \frac{17e^{\eta t}}{4} + \frac{5}{4}\right) + \frac{1}{(e^{\eta t}-1)^{\frac{1}{\eta}}}\right] \tag{57}$$

$$\rho = \frac{-1}{(8\pi+2\mu)}\left\{\left(\frac{1}{1+z}\right)^{-2\eta}\left(\left(\frac{1}{1+z}\right)^{\eta} + 1\right)^2\left(\frac{5\eta}{2} - \frac{17}{4}\left(\frac{1}{1+z}\right)^{\eta} - 3\right) + (1+z)\right\} \tag{58}$$

Pressure as,

$$p = \frac{1}{2\mu}\frac{e^{2\eta t}}{(e^{\eta t}-1)^2}\left[\left(\frac{5\eta}{2} - \frac{17e^{\eta t}}{4} - 1\right) + \frac{\mu}{(8\pi+2\mu)}\left(4\eta - 8e^{\eta t} + \frac{1}{2}\right)\right] + \frac{1}{(8\pi+2\mu)(e^{\eta t}-1)^{\frac{1}{\eta}}} \tag{59}$$

$$p = \frac{1}{2\mu}\left(\frac{1}{1+z}\right)^{-2\eta}\left(\left(\frac{1}{1+z}\right)^{\eta} + 1\right)^2\left\{\left(\frac{5\eta}{2} - \frac{17}{4}\left(\frac{1}{1+z}\right)^{\eta} - \frac{21}{4}\right) + \frac{\mu}{(8\pi+2\mu)}\left(4\eta - 8\left(\frac{1}{1+z}\right)^{\eta} - \frac{15}{2}\right)\right\} + \frac{1+z}{(8\pi+2\mu)} \tag{60}$$

Equation of state parameter is given by,

$$\omega = \frac{p}{\rho}$$

$$\omega = \frac{\frac{1}{2\mu}\frac{e^{2\eta t}}{(e^{\eta t}-1)^2}\left[\left(\frac{5\eta}{2} - \frac{17e^{\eta t}}{4} - 1\right) + \frac{\mu}{(8\pi+2\mu)}\left(4\eta - 8e^{\eta t} + \frac{1}{2}\right)\right] + \frac{1}{(8\pi+2\mu)(e^{\eta t}-1)^{\frac{1}{\eta}}}}{\frac{-1}{(8\pi+2\mu)}\left[\frac{e^{2\eta t}}{(e^{\eta t}-1)^2}\left(\frac{5\eta}{2} - \frac{17e^{\eta t}}{4} + \frac{5}{4}\right) + \frac{1}{(e^{\eta t}-1)^{\frac{1}{\eta}}}\right]} \tag{61}$$

$$\omega = \frac{\frac{1}{2\mu}\left(\frac{1}{1+z}\right)^{-2\eta}\left(\left(\frac{1}{1+z}\right)^{\eta} + 1\right)^2\left\{\left(\frac{5\eta}{2} - \frac{17}{4}\left(\frac{1}{1+z}\right)^{\eta} - \frac{21}{4}\right) + \frac{\mu}{(8\pi+2\mu)}\left(4\eta - 8\left(\frac{1}{1+z}\right)^{\eta} - \frac{15}{2}\right)\right\} + \frac{1+z}{(8\pi+2\mu)}}{\frac{-1}{(8\pi+2\mu)}\left\{\left(\frac{1}{1+z}\right)^{-2\eta}\left(\left(\frac{1}{1+z}\right)^{\eta} + 1\right)^2\left(\frac{5\eta}{2} - \frac{17}{4}\left(\frac{1}{1+z}\right)^{\eta} - 3\right) + (1+z)\right\}} \tag{62}$$

5.2. *Domain wall*

Eqs. (31), (32), and (33) give the energy density and pressure by,

$$\rho = \chi \frac{e^{2\eta t}}{(e^{\eta t}-1)^2}\left[\pi(34\, e^{\eta t} - 20\eta + 8) + \mu\left(\frac{19e^{\eta t}}{4} - \frac{7\eta}{2} + \frac{5}{4}\right)\right] + \chi \frac{\mu}{(e^{\eta t}-1)^{\frac{1}{\eta}}} \tag{63}$$

$$\rho = \chi \left(\frac{1}{1+z}\right)^{-2\eta}\left(\left(\frac{1}{1+z}\right)^{\eta} + 1\right)^2\left[\pi\left(34\,\left(\frac{1}{1+z}\right)^{\eta} - 20\eta + 42\right) + \mu\left(\frac{19}{4}\left(\frac{1}{1+z}\right)^{\eta} - \frac{7\eta}{2} + 6\right)\right] + \chi\mu(1+z) \tag{64}$$

where, $\chi = \frac{-1}{(2\pi+\mu)(32\pi+8\mu)}$

Pressure,

$$p = \frac{e^{2\eta t}}{\mu(e^{\eta t}-1)^2}\left\{\frac{-9}{4} + \psi\left[\pi(34\, e^{\eta t} - 20\eta + 8) + \mu\left(\frac{19e^{\eta t}}{4} - \frac{7\eta}{2} + \frac{5}{4}\right)\right]\right\} + \frac{(\psi.\mu-1)}{\mu(e^{\eta t}-1)^{\frac{1}{\eta}}} \tag{65}$$

$$p = \left(\frac{1}{1+z}\right)^{-2\eta}\left(\left(\frac{1}{1+z}\right)^{\eta} + 1\right)^2 \frac{1}{\mu}\left\{\frac{-9}{4} + \psi\left[\pi\left(34\,\left(\frac{1}{1+z}\right)^{\eta} - 20\eta + 42\right) + \mu\left(\frac{19}{4}\left(\frac{1}{1+z}\right)^{\eta} - \frac{7\eta}{2} + 6\right)\right]\right\} + (1+z)(\psi - \frac{1}{\mu}) \tag{66}$$

where, $\psi = \frac{(8\pi+5\mu)}{(2\pi+\mu)(32\pi+8\mu)}$

Equation of state parameter is given by,

$$\omega = \frac{\frac{e^{2\eta t}}{\mu(e^{\eta t}-1)^2}\left\{\frac{-9}{4}+\psi\left[\pi(34\, e^{\eta t}-20\eta+8)+\mu\left(\frac{19e^{\eta t}}{4}-\frac{7\eta}{2}+\frac{5}{4}\right)\right]\right\}+\frac{(\psi.\mu-1)}{\mu(e^{\eta t}-1)^{\frac{1}{\eta}}}}{\chi\frac{e^{2\eta t}}{(e^{\eta t}-1)^2}\left[\pi(34\, e^{\eta t}-20\eta+8)+\mu\left(\frac{19e^{\eta t}}{4}-\frac{7\eta}{2}+\frac{5}{4}\right)\right]+\chi\frac{\mu}{(e^{\eta t}-1)^{\frac{1}{\eta}}}} \tag{67}$$

$$\omega = \frac{\left(\frac{1}{1+z}\right)^{-2\eta}\left(\left(\frac{1}{1+z}\right)^{\eta}+1\right)^2\frac{1}{\mu}\left\{\frac{-9}{4}+\psi\left[\pi\left(34\,\left(\frac{1}{1+z}\right)^{\eta}-20\eta+42\right)+\mu\left(\frac{19}{4}\left(\frac{1}{1+z}\right)^{\eta}-\frac{7\eta}{2}+6\right)\right]\right\}+(1+z)(\psi-\frac{1}{\mu})}{\chi\left(\frac{1}{1+z}\right)^{-2\eta}\left(\left(\frac{1}{1+z}\right)^{\eta}+1\right)^2\left[\pi\left(34\,\left(\frac{1}{1+z}\right)^{\eta}-20\eta+42\right)+\mu\left(\frac{19}{4}\left(\frac{1}{1+z}\right)^{\eta}-\frac{7\eta}{2}+6\right)\right]+\chi\mu(1+z)} \tag{68}$$

6. Observations from Figures

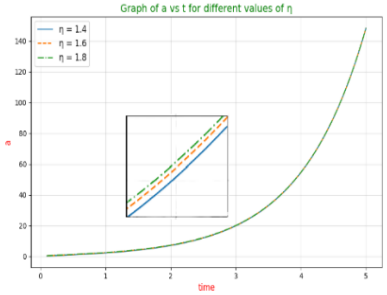

Fig. 1. Variations of average scale factor with respect to cosmic time.

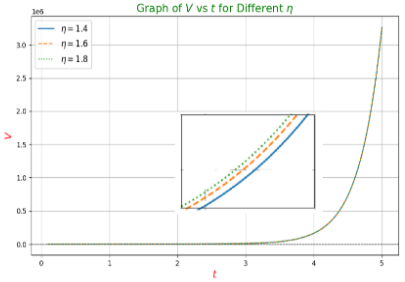

Fig. 2. Variations of Volume with respect to cosmic time.

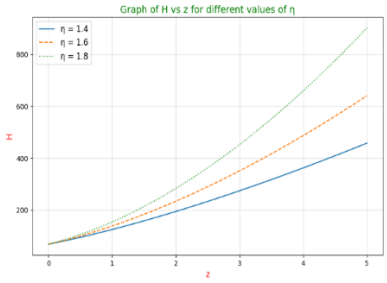

Fig. 3. Variations of Hubble parameter with respect to Redshift.

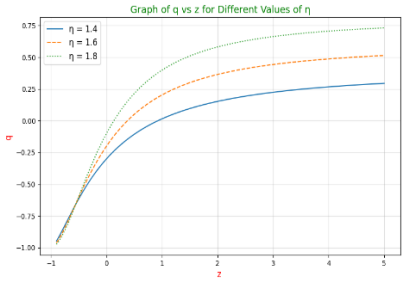

Fig. 4. Variations of deceleration parameter with respect to Redshift.

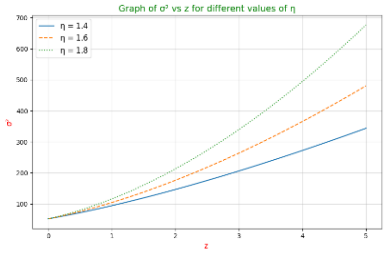

Fig. 5. Variations of Shear scalar with respect to Redshift.

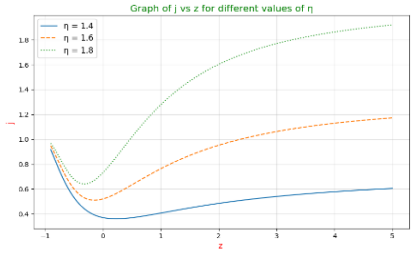

Fig. 6. Variations of jerk parameter with respect to Redshift.

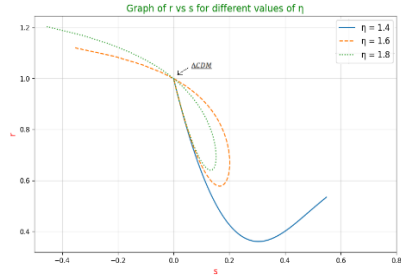

Fig 7. Evolution trajectory of $r - s$ plane

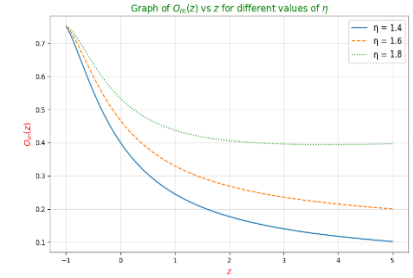

Fig 8. Evolution of $O_m(z)$ with respect to Redshift.

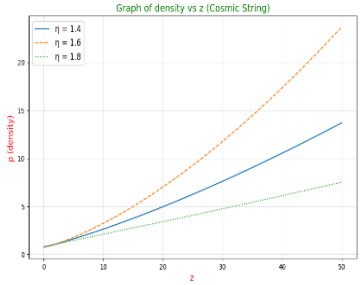

Fig. 9. Variations of density (Cosmic String) with respect to Redshift.

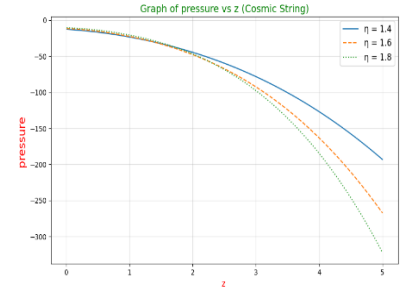

Fig. 10. Variations of pressure (Cosmic String) with respect to Redshift.

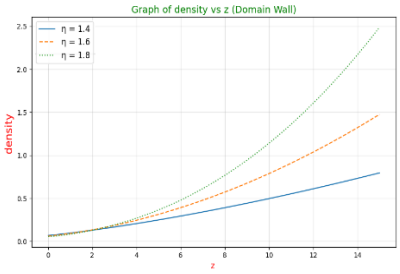

Fig. 11. Variations of density (Domain Wall) with respect to Redshift.

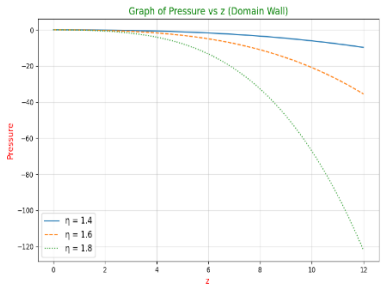

Fig. 12. Variations of pressure (Domain Wall) with respect to Redshift.

Figs. 1 and 2 clearly show that the average scale factor and spatial volume remain steady at the initial time (t = 0). However, as time progresses, both begin to steadily and consistently grow, eventually extending toward infinite values over extended period. This noteworthy observation highlights the present model exhibit continuous expansion.

Fig. 3 illustrates that the Hubble parameter H decreases with the progression of cosmic time. Also, the expansion scalar (θ) is the decreasing function of time, i.e. increasing function with respect to redshift. The value of Hubble parameter is throughout positive. At the present time, the value of Hubble parameter is $H_0 \approx 68$ kms^{-1} Mpc^{-1}.

Fig. 4 demonstrates the transitional behavior of the deceleration parameter. Initially, $q \geq 0$ during the early stages, indicating the decelerating phase of the Universe's expansion. However, as time progresses to the present and into the future, $q < 0$, signifying a shift to an accelerating phase. This transition is consistent with the predictions of the ΛCDM model. Our model shows decelerating to accelerating phase. Also, from graph we get the present value of the deceleration parameter is $q_0 = -0.31$ for η = 1.4, $q_0 = -0.21$ for η = 1.6 and $q_0 = -0.11$ for η = 1.8 respectively

Fig. 5 shows that the shear scalar increases with redshift i.e. shear scalar declines progressively with time and approaches zero for large time values. The shear scalar quantifies the degree of anisotropy in the cosmic expansion. A decreasing shear scalar indicates that the anisotropy diminishes over time, suggesting that the Universe transitions toward a more isotropic state as it evolves.

Fig. 6 illustrates that the jerk parameter (j) remains consistently positive across the entire redshift range for all values of η. This persistent positivity signifies the Universe's ongoing acceleration. As $z \to -1$, the values of j for each η converge towards the expected behavior of the ΛCDM model, highlighting the compatibility of the model with observational data.

Fig. 7 represents the $r - s$ plane serves as a valuable graphical tool for mapping and distinguishing between various dark energy models and cosmological scenarios. Each point on this plane represents a unique cosmological model, providing a visual framework for understanding their distinct characteristics.

a. (r = 1, s = 0): ΛCDM
b. (r = 1, s = 1): SCDM
c. (r = 1, s = $\frac{2}{3}$): Holographic dark energy

d. (r > 1, s < 0): Phantom region
e. (r < 1, s > 0): Quintessence region

The coordinates (1,0) on the $r - s$ plane represent the standard ΛCDM model, where dark energy is described as a cosmological constant (Λ) and cold dark matter (CDM) constitutes the dominant matter component of the Universe. The $r - s$ plane proves to be a highly effective tool for examining the trajectories of various dark energy models, offering valuable insights into their distinctive properties, such as evolutionary dynamics and deviations from the ΛCDM framework. For example, quintessence, a dynamic form of dark energy driven by a scalar field, is located to the right of the ΛCDM model at η=1.4 in the $r - s$ plane. This positioning highlights the unique evolutionary characteristics of quintessence, which may include a time-dependent equation of state and potential departures from the conventional ΛCDM model.

A constant $O_m(z)$ indicates that dark energy is a cosmological constant, while a positive slope suggests phantom $(\omega < -1)$ behaviour and negative slope suggest quintessence $(\omega > -1)$ behavior respectively. Fig 8 shows that $O_m(z)$ increases as z decreases, i.e. $O_m(z)$ decreases with redshift. The decreasing trend of $O_m(z)$ with redshift indicates a quintessence-like behavior of dark energy, characterized by an equation of state parameter $(\omega > -1)$. Such a trend supports the notion of a time-dependent dark energy component driving the accelerated expansion of the Universe.

Figs. 9 and 11 show the energy density in both cosmic string and domain wall respectively. From both the graphs we can say that the energy density starts with a significant value and displays the Fascinating trend and gradually decreases over time, eventually approaching zero in the present and future. This clear pattern provides strong evidence of the Universe's continuous expansion.

Figs. 10 and 12 graph demonstrate the influence of topological defects (cosmic strings and domain walls) on the pressure evolution. From both the graphs we can say that the analysis reveals that the pressure transitions from significantly large negative values to slightly negative values over time, eventually approaching zero as t→∞. This persistent negativity in pressure highlights the presence of dark energy, a fundamental driver of the Universe's accelerated expansion.

7. Conclusions

The present study focuses on an accelerating model of the Universe formulated in the context of $f(R,T)$ gravity. In the course of our investigation, we establish field equations for anisotropic Bianchi type III cosmological model in the presence of Cosmic string and Domain wall. Utilizing a special form of deceleration parameter, we deduce cosmological solutions that exhibit remarkable similarity to the properties of the ΛCDM model influenced by dark energy. Our study findings lead to the following conclusions:

Initially, at $t = 0$ the average scale factor and spatial volume is finite but as $t \to \infty$, both average scale factor and spatial volume become infinite. Here average scale factor and spatial volume show expanding model with time t. It has been noted that the Hubble parameter H remain positive and gradually approach zero as time progresses towards

infinity. The positivity of the Hubble parameter signifies the ongoing expansion of the Universe. Also, $\frac{\sigma^2}{\theta^2}$ = Constant ≠ 0, and hence the model does not approach isotropy for large values of t. Our results demonstrate that, over time, the deceleration parameter (q), as defined in Eq. (42), transitions from positive to negative values and eventually approaches −1. This behavior aligns with the features of the dark energy-dominated ΛCDM model. As a result, our Universe model exhibits a shift from an initial decelerating phase to the present accelerating phase, a conclusion that is consistent with recent observational data.

The cosmic jerk parameter remains positive throughout and converges to unity at late times, aligning with observational data and supporting the ΛCDM model. The analysis of statefinder parameters yields $\{r, s\} = \{1, 0\}$, strongly supporting the ΛCDM model and its consistency with recent observations. Additionally, the ΛCDM model positions quintessence to the right in the {r, s} plane, highlighting its distinct evolutionary behavior. The decreasing trend of $O_m(z)$ with redshift indicates a quintessence-like behavior of dark energy, characterized by an equation of state parameter $(\omega > -1)$. The density (ρ) increases with redshift (z) for both domain walls and cosmic strings, showing their stronger influence in the early Universe. Higher η values lead to steeper growth. Pressure decreases with redshift for all η, remaining negative-indicating a repulsive effect responsible for the Universe's accelerated expansion due to dark energy or topological defects.

References

1. A. G. Riess, A. V. Filippenko, P. Challis, A. Clocchiatti, A. Diercks, P. M Garnavich, et al., The Astronom. J. **116**, 1009 (1998). https://doi.org/10.1086/300499
2. S. Perlmutter, G. Aldering, G. Goldhaber, R. A. Knop, P. Nugent, P. G. Castro, S. Deustua, et al., The Astrophys. J. **517**, 565 (1999). https://doi.org/10.1086/307221
3. A. G. Riess, L.-G. Strolger, J. Tonry, S. Casertano, H. C. Ferguson, B. Mobasher et al., The Astrophys. J. **607**, 665 (2004). https://doi.org/10.1086/383612
4. C. L. Bennett, A. J. Banday, K. M. Górski, G. Hinshaw, P. Jackson et al., The Astrophys. J. **464**, ID L1 (1996). https://doi.org/10.1086/310075
5. D. J. Eisenstein, I. Zehavi, D. W. Hogg, R. Scoccimarro, M. R. Blanton, R. C. Nichol, R. Scranton et al., The Astrophys. J. **633**, 560 (2005).
6. W. J. Percival, B. A. Reid, D. J. Eisenstein, N. A. Bahcall, T. Budavari, J. A. Frieman, M. Fukugita et al., Monthly Notices of the Royal Astronom. Soc. **401**, 2148 (2010). https://doi.org/10.1111/j.1365-2966.2009.15812.x
7. D. N. Spergel, L. Verde, H. V. Peiris, E. Komatsu, M. R. Nolta, C. L. Bennett, M. Halpern et al., The Astrophys. J. Supplement Series **148**, 175 (2003). https://doi.org/10.1086/377226
8. T. Koivisto and D. F Mota, Phys. Rev. D **73**, ID 083502 (2006). https://doi.org/10.1103/PhysRevD.73.083502
9. S. F. Daniel, R. R. Caldwell, A. Cooray, and A. Melchiorri, Phys. Rev. D **77**, ID 103513 (2008). https://doi.org/10.1103/PhysRevD.77.103513
10. M. Colless, G. Dalton, S. Maddox, W. Sutherland, P. Norberg, S. Cole, J. Bland-Hawthorn et al., Monthly Notices of the Royal Astronom. Soc. **328**, 1039 (2001). https://doi.org/10.1046/j.1365-8711.2001.04902.x
11. C. L. Bennett, M. Bay, M. Halpern, G. Hinshaw, C. Jackson, N. Jarosik, A. Kogut et al., The Astrophys. J. **583**, 1 (2003). https://doi.org/10.1086/345346
12. R. R. Caldwell and M. Doran, Phys. Rev. D **69**, ID 103517 (2004). https://doi.org/10.1103/PhysRevD.69.103517
13. A. Vilenkin, Phys. Rev. D **23**, 852 (1981). https://doi.org/10.1103/PhysRevD.23.852

14. P. S. Letelier, Phys. Rev. D **28**, 2414 (1983). https://doi.org/10.1103/PhysRevD.28.2414
15. J. Satchel, Phys. Rev. D **21**, 2171 (1980). https://doi.org/10.1103/PhysRevD.21.2171
16. K. S. Adhav, A. S. Nimkar, and M. V. Dawande, Astrophys. Space Sci. **310**, 231 (2007). https://doi.org/10.1007/s10509-007-9506-8
17. K. S. Adhav, A. S. Nimkar, H. R.Ghate, Rom. J. Phys. **53**, 909 (2008).
18. D. R. K. Reddy, Astrophys. Space Sci. **286**, 365 (2003). https://doi.org/10.1023/A:1026322816690
19. D. R. K. Reddy, Astrophys. Space Sci. **286**, 397 (2003). https://doi.org/10.1023/A:1026397732469
20. D. R. K. Reddy, R. L. Naidu, and V. U. M. Rao, Astrophys. Space Sci. **306**, 185 (2006). https://doi.org/10.1007/s10509-006-9169-x
21. D. R. K. Reddy and R. L. Naidu, Astrophys. Space Sci. **307**, 395 (2007). https://doi.org/10.1007/s10509-007-9387-x
22. R. Venkateswarlu, V. U. M. Rao, and K. Pavankumar, Int. J. Thoer. Phys. **47**, 640 (2008). https://doi.org/10.1007/s10773-007-9488-x
23. V. U. M. Rao, M. V. Santhi, T. Vintha, Astrophys. Space sci. **314**, 73 (2008). https://doi.org/10.1007/s10509-008-9739-1
24. S. D. Katore, A. Y. Shaikh, M. M. Sancheti, and N. K. Sarkate, Prespacetime J. **2**, 447 (2011).
25. R. L. Naidu, D. R. K. Reddy, T. Ramprasad, and K. V. Ramana, Astrophys. Space Sci. **348**, 247 (2013). https://doi.org/10.1007/s10509-013-1540-0
26. D. R. K Reddy, S. Babu, and P. Raju, Astrophys. Space Sci. **353**, 275 (2014). https://doi.org/10.1007/s10509-014-2024-6
27. D. D. Pawar, S. N. Bayaskar, and A. G. Deshmukh, Rom. J. Phys. **56**, 842 (2011).
28. K. Pawar and A. K. Dabre, J. Sci. Res. **15**, 695 (2023). https://doi.org/10.3329/jsr.v15i3.64173
29. V. R. Chirde, S. P. Hatkar, and S. D. Katore, Int. J. Mod. Phys. D **29**, ID 2050054 (2020). https://doi.org/10.1142/S0218271820500546
30. S. R. Bhoyar, V. R. Chirde, and S. H. Shekh, J. Sci. Res. **11**, 249 (2019). https://doi.org/10.3329/jsr.v11i3.39220
31. D. D. Pawar, S. N. Bayaskar, and V. R. Patil, Bulg. J. Phys. **36**, 68 (2009).
32. K. Saikawa, Universe **3**, ID 40 (2017). https://doi.org/10.3390/universe3020040
33. D. R. K. Reddy and M. V. S. Rao, Astrophys. Space Sci. **302**, 157 (2006). https://doi.org/10.1007/s10509-005-9022-7
34. K. S. Adhav, A. S. Nimkar, and R. L. Naidu, Astrophys. Space Sci. **312**, 165 (2007). https://doi.org/10.1007/s10509-007-9670-x
35. D. R. K.Reddy, P. G. Rao, and R. L. Naidu, Int. J. Theor. Phys. **47**, 2966 (2008). https://doi.org/10.1007/s10773-008-9731-0
36. V. U. M. Rao and U. Y. D. Prasanthi, Prespacetime J. **7** (2016).
37. S. P. Hatkar, D. P. Tadas, and S. D. Katore, arXiv preprint arXiv:2410.07657 (2024).
38. S. D. Katore and S. P. Hatkar, Prog. Theoret. Exp. Phys. **2016**, ID 033E01 (2016). https://doi.org/10.1093/ptep/ptw009
39. S. D. Katore, S. P. Hatkar, and R. J. Baxi, Chi. J. Phys. **54**, 563 (2016). https://doi.org/10.1016/j.cjph.2016.05.005
40. S. D. Katore, V. R. Chirde, and S. P. Hatkar, Inter J. Theoret. Phys. **54**, 3654 (2015). https://doi.org/10.1007/s10773-015-2602-6
41. S. P. Hatkar, D. P. Tadas, and S. D. Katore, General Relativity and Quantum Cosmology (2023). https://doi.org/10.48550/arXiv.2305.10970
42. U. K. Sharma, A. K. Mishra, and A. Pradhan, Canadian J. Phys. **99**, 378 (2021). https://doi.org/10.1139/cjp-2020-0343
43. J. L. Pawde, R. Mapari, V. Patil, and D. Pawar, Eur. Phys. J. C **84**, 320 (2024). https://doi.org/10.1140/epjc/s10052-024-12646-4
44. P. K. Sahoo and B. Mishra, J. Theoret. Appl. Phys. **7** (2013). https://doi.org/10.1186/2251-7235-7-62

45. K. L. Mahanta and A. K. Biswal, J. Mod. Phys. **3**, 1479 (2012). https://doi.org/10.4236/jmp.2012.310182
46. S. D. Katore, A. Y. Shaikh, M. M. Sancheti, and N. K. Sarkate. Prespacetime J. **2**, 447 (2011).
47. A. K. Singha, U. Debnath, Int. J. Theor. Phys. **48**, 351 (2009). https://doi.org/10.1007/s10773-008-9807-x
48. V. R. Chirde and S. H. Shekh, Astrophys. **58**, 106 (2015). https://doi.org/10.1007/s10511-015-9369-6
49. P. K. Sahoo, P. Sahoo, and B. K. Bishi, Int. J. Geom. Meth. Mod. Phys. **14**, ID 1750097 (2017). https://doi.org/10.1142/S0219887817500979
50. T. Harko, F. S. N. Lobo, S. Nojiri, and S. D. Odintsov, Phys. Rev. D **84**, ID 024020 (2011). https://doi.org/10.1103/PhysRevD.84.024020
51. P. S. Letelier, Phys. Rev. D **20**, 1294 (1979). https://doi.org/10.1103/PhysRevD.20.1294
52. V. Sahni, A. Shafieloo, and A. A. Starobinsky, Phys. Rev. D **78**, ID 103502 (2008). https://doi.org/10.1103/PhysRevD.78.103502
53. V. G. Mete and V. Deshmukh. J. Sci. Res. **15**, 351 (2023). http://dx.doi.org/10.3329/jsr.v15i2.61442
54. V. G. Mete, V. S. Deshmukh, and D. V. Kapse, J. Sci. Res. **16**, 479 (2024). http://dx.doi.org/10.3329/jsr.v16i2.68364
55. S. N. Bayaskar, A. A. Q. Shoeb, A. A. Dhanagare, and U. T. Arbat, J. Astrophys. Astronom. **46**, ID 66 (2025). https://doi.org/10.1007/s12036-025-10089-1
56. M. R. Ugale and S. B. Deshmukh, J. Sci. Res. **16**, 17 (2024). http://dx.doi.org/10.3329/jsr.v16i1.62830